

# STRUCTURE OF GALAXIES

## 9. Elliptical galaxies

Piet van der Kruit  
Kapteyn Astronomical Institute  
University of Groningen  
the Netherlands

February 2010

## Outline

### Surface photometry

- Luminosity distributions
- Shells and ripples
- Color gradients

### Dynamics

- Dynamical models
- Fundamental Plane
- $V_m/\bar{\sigma} - \epsilon$  relation and tri-axiality
- Detailed kinematics
- Central kinematics and black holes
- Stackel potentials
- Dark matter

### Formation

# Surface photometry

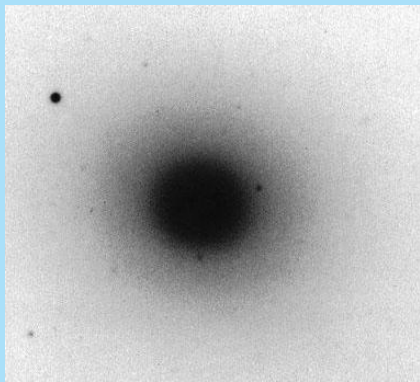
## Luminosity distributions

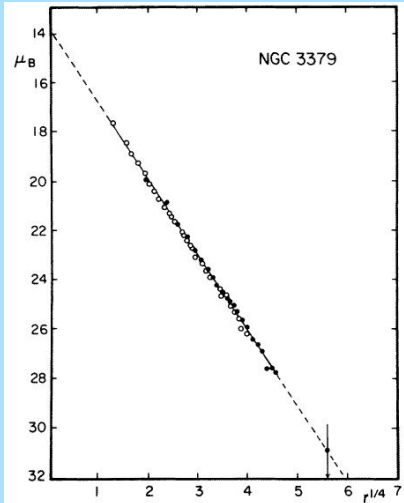
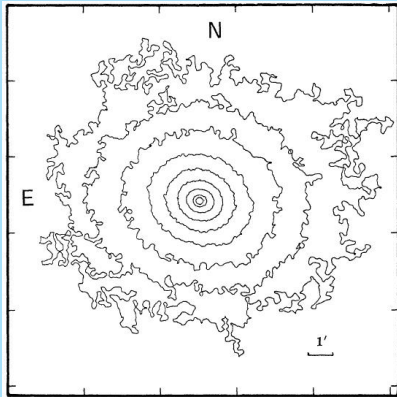
Elliptical galaxies usually conform to the  $R^{1/4}$ -law and look smooth and regular.

NGC 3379 has been used as a prototype and standard for surface photometry<sup>a</sup>.

---

<sup>a</sup>G. de Vaucouleurs & M. Capaccioli, Ap.J.Suppl. 40, 699 (1979)





Detailed study shows that the isophotal structure of ellipticals is usually much more complicated.

In particular there are **isophote twists** and **deviations from ellipticity**.

The latter are described by parameters  $a(i)$ .

These describe the deviations from pure ellipses in multiplicity  $i^1$ . These are derived from Fourier analysis of the isophote shapes relative to the best fitting ellipse.

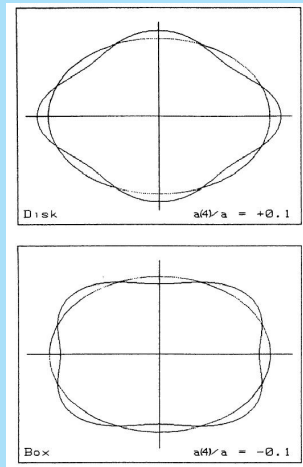
By definition (because of the ellipse fit)  $a(i) = 0$  for  $i = 0, 1, 2$ .

---

<sup>1</sup>R. Bender, S. Döbereiner & C. Möllenhoff, A.&A.Suppl. 74, 385 (1988)

The most interesting is  $a(4)$ , which is **negative** for “boxy” isophotes and **positive** for “disky” isophotes.

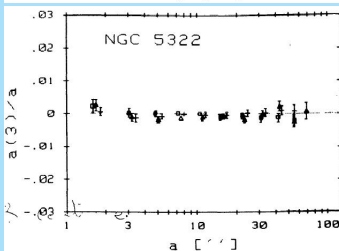
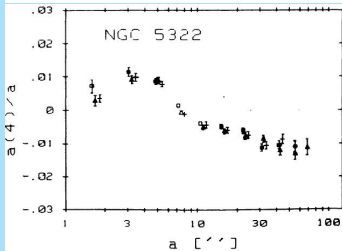
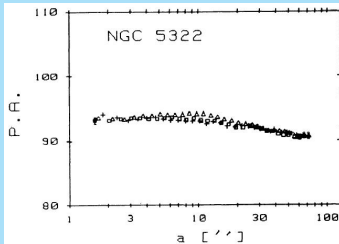
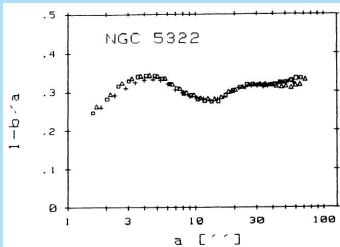
Here are some examples of non-zero parameters  $a(4)$ .



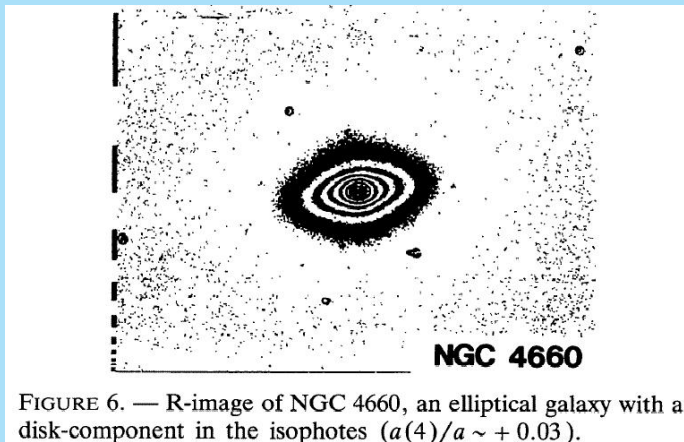
We will now look at fits in a boxy galaxy.

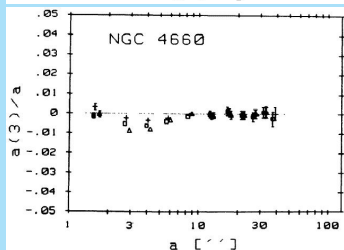
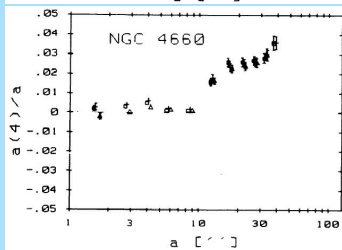
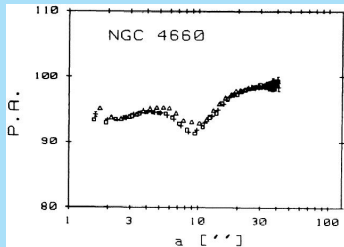
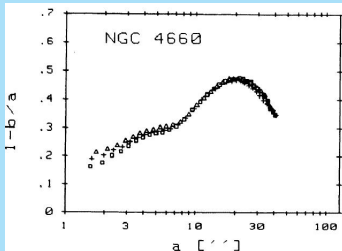


FIGURE 7. — R-image of NGC 5322, an elliptical galaxy with box-shaped isophotes ( $a(4)/a \sim -0.01$ ).



And here are fits a disk galaxy.





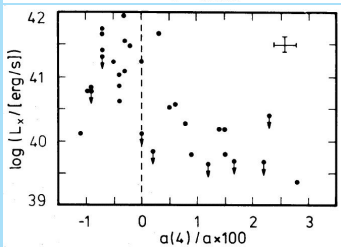
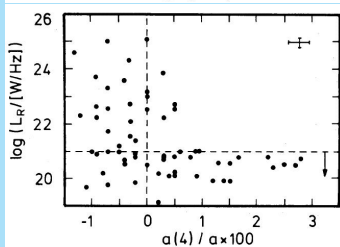
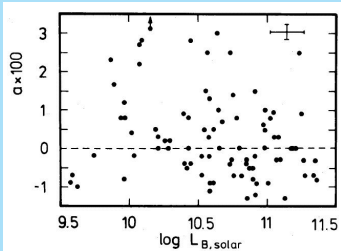
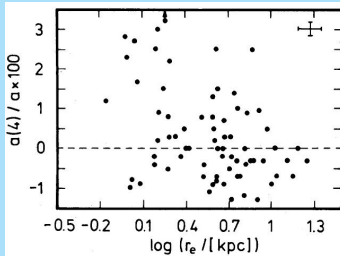
The global  $a(4)$  parameter for a sample of galaxies does not correlate with **effective radius** or **integrated luminosity**<sup>2</sup>.

However, galaxies with strong **radio emission** or **X-ray halo's** are almost always boxy.

It has been suggested that “boxyness” results from **interactions**.

---

<sup>2</sup>R. Bender, P. Surma, S. Döbereiner, C. Möllenhoff & R. Madejsky, A.&A. 217, 35 (1989)



There is a well-defined **color – magnitude relation** for early-type galaxies<sup>3</sup>.

The relation is the same in clusters and in the field.

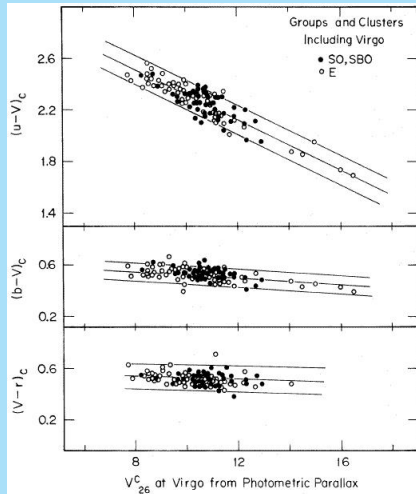
It is actually one between **metallicity** and **mass** (or **escape velocity**).

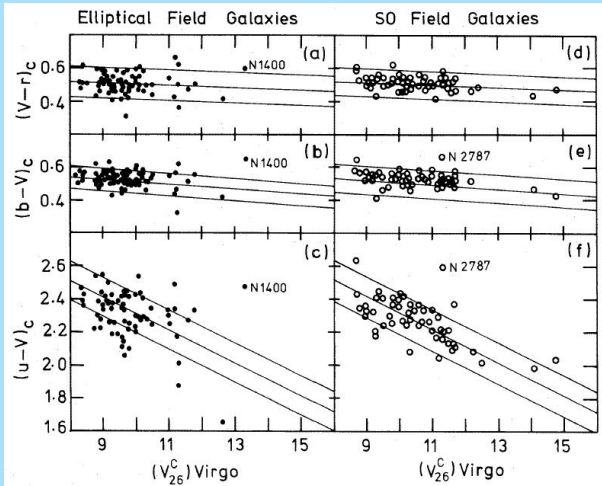
---

<sup>3</sup>A. Sandage, Ap.J. 176, 21 (1972)

N, Visvanathan & A. Sandage, Ap.J. 216, 214 (1977)

A. Sandage & N. Visvanathan, Ap.J. 223, 707 and 225, 742 (1978)



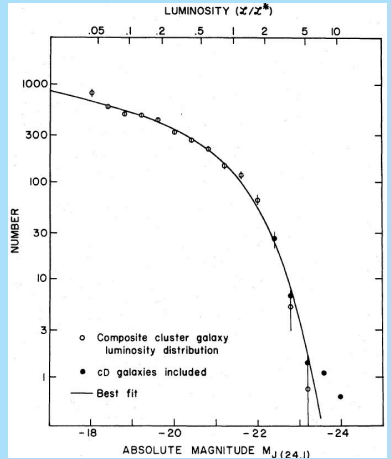


The luminosity function of galaxies is fitted with the Schechter-function<sup>a</sup>

$$\phi(L)dL \propto (L/L^*)^\alpha \exp(-L/L^*)d(L/L^*)$$

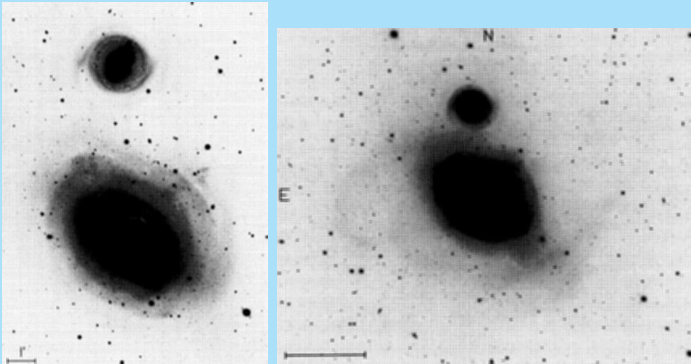
The best fits have  $\alpha \sim 1.2$  and  $L^*$  corresponding to  $M_B^* \sim -20.6$ .

<sup>a</sup>P. Schechter, Ap.J. 203, 297 (1976)



## Shells and ripples

In the outer parts faint “shells and ripples” are seen, such as in NGC 1316 = Fornax A<sup>4</sup>.



<sup>4</sup>F. Schweizer, Ap.J. 237, 303 (1980)

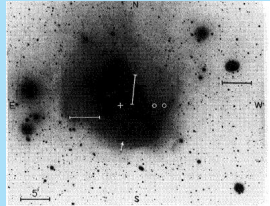
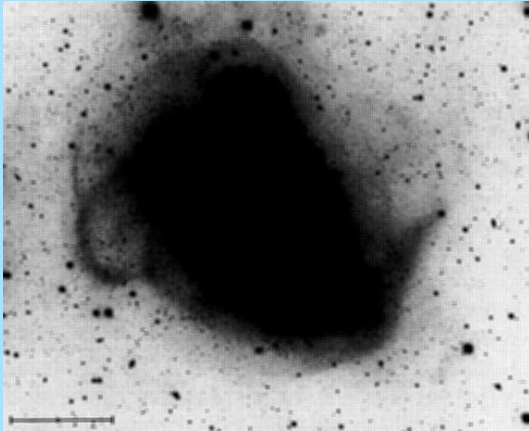
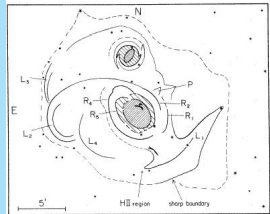


Fig. 1



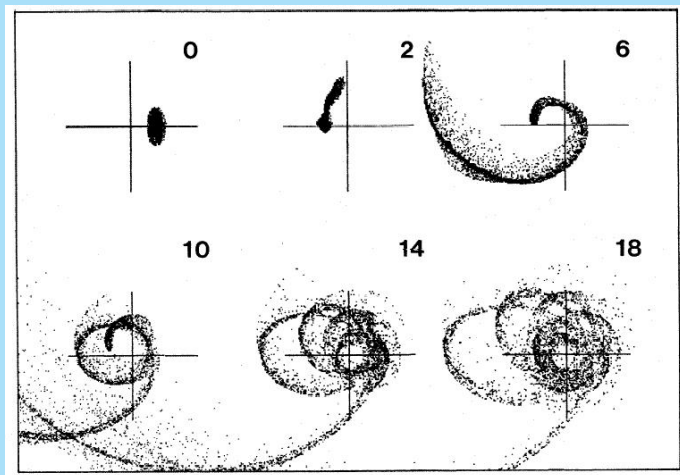
Numerical experiments<sup>5</sup> show that these can be the result of a collision with a disk galaxy.

In the figure on the next frame we see how the disk evolves in the potential of a 100 times more massive elliptical galaxy in a typical encounter.

The unit of time is the circular period at a characteristic radius in the potential.

---

<sup>5</sup>P.J. Quinn, Ap.J. 279, 596 (1984)

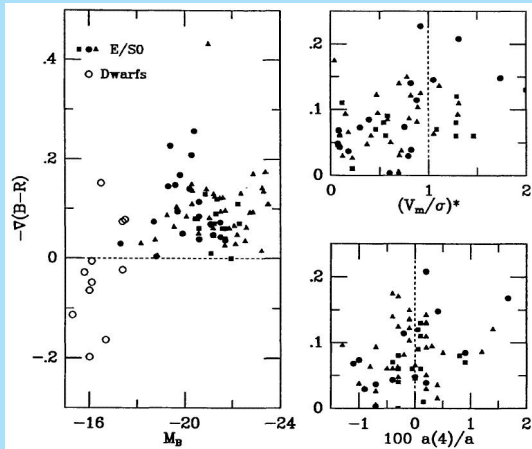


## Color gradients

Important for formation models is the correlation of **color gradients** with structural and dynamical properties.

**Color gradients** usually are defined as the change in color index in magnitudes per decade in radius or

$$\nabla(B - V) = \Delta(B - V) / \Delta(\log r).$$



The property  $(V_m/\sigma)^*$  is normalised to unity for an isotropic oblate rotator.

- ▶ Ellipticals have significant color gradients. The light becomes **redder towards the center**.
- ▶ However, **dwarf spheroidals** have inverse gradients. This may be due to recent star formation.
- ▶ **Anisotropic** galaxies have **smaller** gradients.
- ▶ Also **boxy** galaxies tend to have **smaller** gradients.
- ▶ There is **no strong correlation** between the strength of the color gradient and the luminosity or velocity dispersion.

# Dynamics

## Dynamical models

The **isothermal sphere** has at large  $R$

$$\rho(R) = \frac{\langle V^2 \rangle}{2\pi G} R^{-2}$$

The **core radius** is

$$r_o = \left( \frac{4\pi G \rho_o}{9\langle V^2 \rangle} \right)^{-1/2}$$

For a better description we need **King-models**<sup>6</sup>. For these introduce **tidal radius**  $R_t$ , then

$$\langle V^2 \rangle^{1/2} \propto \rho_o M(R_t) f \left( \frac{R_t}{r_o} \right)$$

with  $f(R_t/r_o)$  some numerical function. The central surface density is

$$\sigma_o = \rho_o r_o g \left( \frac{R_t}{r_o} \right)$$

with  $g(R_t/r_o)$  another numerical function.

For ellipticals  $\log(R_t/r_o) \approx 2.2$ .

---

<sup>6</sup>King, A.J. 67, 471 (1962)

## Fundamental Plane

With Fish's law (constant central surface brightness) and constant  $M/L$  then follows the **Faber-Jackson relation**<sup>7</sup> between **luminosity**  $L$  and **stellar velocity dispersion**  $\sigma$ :

$$L \propto \sigma^4$$

There is also a relation between **diameter**  $D_\Sigma$  (the radius at which the mean surface brightness is  $20.75 \text{ mag arcsec}^{-2}$ ) and the **velocity dispersion**<sup>8</sup>:

$$D_\Sigma \propto \sigma^{4/3}$$

---

<sup>7</sup>S.M. Faber & R.E. Jackson, Ap.J. 204, 668 (1976)

<sup>8</sup>A. Dressler *et al.*, Ap.J. 313, 42 (1987)

This can be used to decrease the scatter in the FJ-relation by including **surface brightness** ( $\langle SB_e \rangle =$  mean surface brightness within the effective radius) as a second parameter

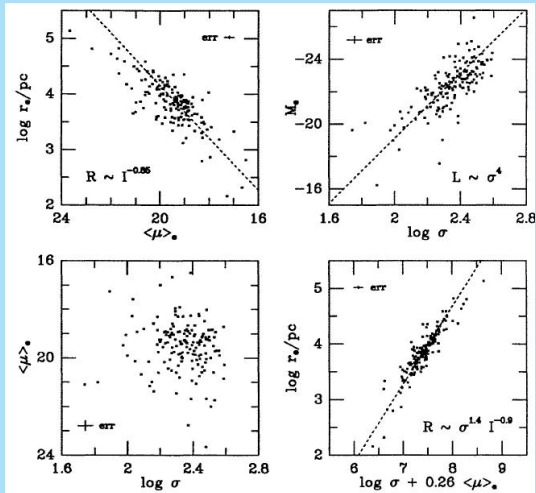
$$L \propto \sigma^{2.65} \langle SB_e \rangle^{-0.65}.$$

The “**fundamental plane**” of elliptical galaxies is a relation between some consistently defined **radius** (e.g. core radius)  $R$ , the observed **central velocity dispersion**  $\sigma$  and a consistently defined **surface brightness**  $I^9$ :

$$R \propto \sigma^{1.4 \pm 0.15} I^{-0.9 \pm 0.1}$$

---

<sup>9</sup>see J. Kormendy & G. Djorgovski, Ann.Rev.Astron.Astrophys. 27, 235 (1989)



In broad terms the **Fundamental Plane** can be understood as follows.

For equilibrium the **Virial Theorem** states that

$$2T_k + \Omega = 0$$

where  $T_k$  is the total **kinetic energy** and  $\Omega$  the **potential energy**.

The kinetic energy is proportional to  $MV^2$  and the potential energy to  $M^2/R$ . Here  $M$  is the total mass,  $V$  a typical internal velocity and  $R$  some characteristic radius.

All the information on the detailed density and velocity structure is in the proportionality constants.

Thus we have<sup>10</sup>

$$M \propto RV^2$$

For elliptical galaxies the kinetic energy is dominated by that in random motions rather than rotation. So for  $V$  we will take the mean **velocity dispersion**  $\sigma$ .

With the **mass-to-light ratio**  $M/L$ , we replace  $M$  with  $L(M/L)$  with  $L$  the total luminosity.

$R$  remains a typical radius such as the **effective radius**; then we get

$$R \propto L \frac{M}{L} \sigma^2$$

<sup>10</sup>For a disk we take the scalelength  $h$  for  $R$  and the rotation velocity  $V_{\text{rot}}$  for  $V$ . It then easily follows that  $M \propto \sigma_o^{-1} V_{\text{rot}}^4$ , which is the Tully-Fisher relation. 

If  $I$  is the mean **surface brightness** within  $R$  we have  $I \propto LR^{-2}$  and

$$R \propto \sigma^2 I^{-1} \left( \frac{M}{L} \right)^{-1}$$

The coefficients are close to the observed ones. Differences arise because of variations in actual structural parameters and possible dependence of  $M/L$  on  $M$  and/or  $\sigma$ .

## $V_m/\bar{\sigma} - \epsilon$ relation and tri-axiality

Originally elliptical galaxies were thought to be simple systems, mainly supported by random motions and flattened by rotation.

If we consider elliptical galaxies to be oblate spheroids, flattened by rotation we can estimate how much rotation is needed using the virial equation

$$0 = 2T_{ij} + \Pi_{ij} + W_{ij} = 2K_{ij} + W_{ij}$$

$K$  is the kinetic energy consisting of that in ordered motions  $T$  and in random motions  $\Pi$ , and  $W$  is the potential energy.

$$K_{ij} = \int \rho \bar{v}_i \cdot \bar{v}_j d^3x + \frac{1}{2} \int \rho \sigma_{ij}^2 d^3x$$

$$T_{ij} + \frac{1}{2} \Pi_{ij}$$

$$W_{jk} = - \int x_j \frac{\partial \Phi}{\partial x_k} d^3x$$

Let the spheroid be flattened along the  $z$ -axis. Then the symmetry with respect to this axis requires

$$\langle V_R \rangle = \langle V_z \rangle = \langle V_R V_\theta \rangle = \langle V_z V_\theta \rangle = 0$$

The rotational velocity is  $\langle V_\theta \rangle$ .

It can be shown then that *all non-diagonal elements* of the tensors  $T_{ij}$ ,  $\Pi_{ij}$  and  $W_{ij}$  can be shown to be equal to zero.

Then because of *symmetry* in the system we must also have

$$T_{xx} = T_{yy} \quad ; \quad \Pi_{xx} = \Pi_{yy} \quad ; \quad W_{xx} = W_{yy}$$

So the only non-trivial virial equations are

$$2T_{xx} + \Pi_{xx} + W_{xx} = 0 \quad ; \quad 2T_{zz} + \Pi_{zz} + W_{zz} = 0$$

So

$$\frac{2T_{xx} + \Pi_{xx}}{2T_{zz} + \Pi_{zz}} = \frac{W_{xx}}{W_{zz}}$$

To a good approximation, for oblate bodies we have then

$$\frac{2T_{xx} + \Pi_{xx}}{2T_{zz} + \Pi_{zz}} = \frac{W_{xx}}{W_{zz}} \propto \left(\frac{c}{a}\right)^{-0.9}$$

This is treated in detail for those interested in my course on **Dynamics of galaxies**, lecture 8<sup>11</sup>.

Now consider the cases where the system is either rotating or not or has an isotropic or anisotropic velocity distribution.

---

<sup>11</sup>[www.astro.rug.nl/~vdkruit/jea3/homepage/dynamics08.pdf](http://www.astro.rug.nl/~vdkruit/jea3/homepage/dynamics08.pdf)

## A. Isotropic and rotating.

Then the velocity dispersion  $\sigma$  is **independent** of direction. But it may vary with the ellipsoidal surface it is on and therefore we use a density-weighted rms (one-dimensional) velocity dispersion  $\bar{\sigma}$ . So, if the total mass is  $M$

$$\Pi_{xx} = \int \rho \sigma_{xx}^2 d^3x = M \bar{\sigma}^2 = \Pi_{zz}$$

Say, the density-weighted rotation velocity (around the  $z$ -axis) is  $\bar{V}$ ; then  $v_x^2 = \frac{1}{2} \bar{V}^2$ , and we get

$$T_{zz} = 0$$

$$T_{xx} = \frac{1}{2} \int \rho v_x^2 d^3x = \frac{1}{4} M \bar{V}^2 = T_{yy}$$

Therefore

$$\frac{\frac{1}{2}M\bar{V}^2 + M\bar{\sigma}^2}{M\bar{\sigma}^2} = \left(\frac{c}{a}\right)^{-0.9}$$

This can be reduced to

$$\frac{\bar{V}}{\bar{\sigma}} = \sqrt{2 \left[ \left(\frac{c}{a}\right)^{-0.9} - 1 \right]}$$

This is interesting, since it shows that a **large amount of rotation is necessary to give rise to flattening**. E.g. for a rather modest flattening of  $c/a = 0.7$  one needs  $\bar{V} \sim 0.9\bar{\sigma}$ .

## B. Anisotropic and non-rotating

Then  $T_{xx} = 0$  and  $\Pi_{xx} = M\bar{\sigma}_{xx}^2$ ,  $\Pi_{zz} = M\bar{\sigma}_{zz}^2$

This gives

$$\frac{\bar{\sigma}_{zz}}{\bar{\sigma}_{xx}} \sim \left(\frac{c}{a}\right)^{-0.9}$$

For the same modest flattening of  $c/a = 0.7$  one now needs only a small anisotropy  $\bar{\sigma}_{zz}/\bar{\sigma}_{xx} \sim 0.85$ .

## C. Anisotropic and rotating

Write

$$\Pi_{zz} = (1 - \delta)\Pi_{xx} = (1 - \delta)M\bar{\sigma}^2$$

We have again  $T_{zz} = 0$  and  $2T_{xx} = \frac{1}{2}M\bar{V}^2$ .

Then

$$\frac{\bar{V}}{\bar{\sigma}} = \sqrt{2 \left[ (1 - \delta) \left( \frac{c}{a} \right)^{-0.9} - 1 \right]}$$

This would mean that we can expect a relation between  $\bar{V}/\bar{\sigma}$  and the **ellipticity**  $\epsilon = 1 - (c/a)$  in elliptical galaxies.

So, the rotation turns out to be too small to provide the flattening so this had to be due to **anisotropic velocity distributions**.

A parameter used is the ratio of the **observed maximum rotation velocity**  $V_m$  and the **observed line-of-sight velocity dispersion** at the center  $\bar{\sigma}$ .

This is a measure of the **relative importance of rotation and random motions**.

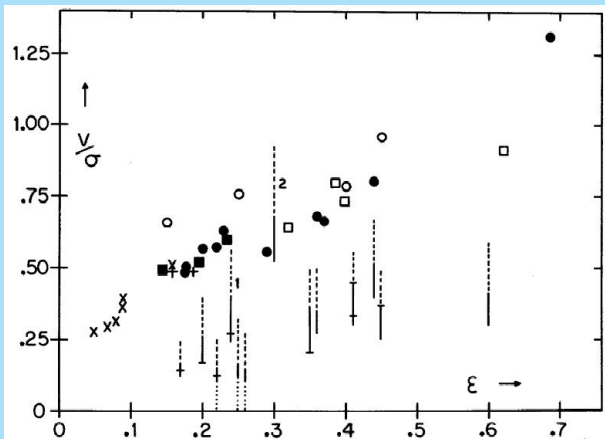
It can be compared to the *observed flattening*  $\epsilon = 1 - b/a$  with  $a$  and  $b$  the (projected) major and minor axis<sup>12</sup>.

The symbols in the next graph indicate models with isotropic velocity dispersions that are flattened by rotation and seen under various inclinations.

The bars are data and rotate less than expected for the observed flattening.

---

<sup>12</sup>G. Illingworth, Ap.J. 218, L43 (1977)



Note that the models lie on a well-defined line where the intrinsic relation roughly coincides with the projected one.

Further work<sup>13</sup> showed that **spiral bulges** and **faint ellipticals** are fast rotators.

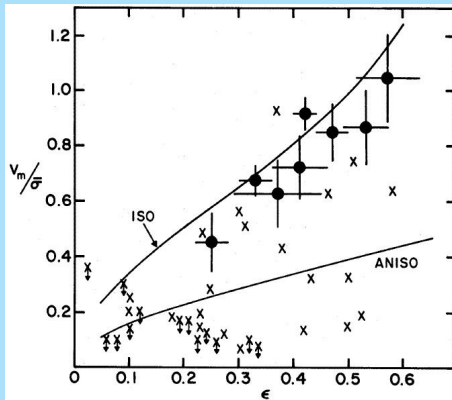
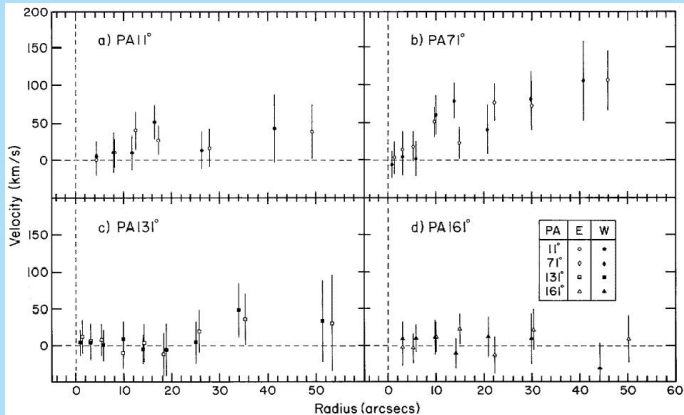


FIG. 3.—Comparison of bulge data (filled circles) with all available elliptical galaxy data (crosses, arrows indicate upper limits) in the dimensionless rotation-ellipticity plane. Derivation of  $V_m$ ,  $\bar{\sigma}$ , and  $\epsilon$  is discussed in the text. The line labeled ISO represents projected models of oblate spheroids with isotropic residual velocities and rotational flattening. The line labeled ANISO describes a typical anisotropic oblate model with  $\sigma_x$  smaller than  $\sigma_y$  and  $\sigma_z$ .

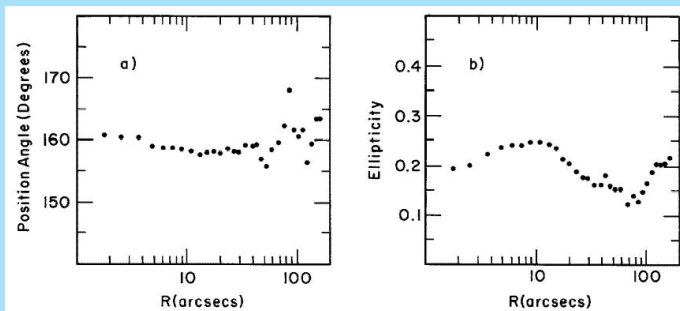
<sup>13</sup>e.g. J. Kormendy & G. Illingworth, Ap.J. 256, 460 (1982)

Minor axis rotation was first discovered in NGC 4261<sup>14</sup>.



<sup>14</sup>R.L. Davies & M. Birkinshaw, Ap.J. 303, L45 (1986)

The maximum rotation is in p.a.  $\sim 70^\circ$ , while the isophotes have major axis at  $\sim 160^\circ$ .



The suggestion was made that this galaxy is **prolate**.

It turned out that elliptical galaxies are **triaxial**<sup>15</sup>.

This explains the  $(V_m/\sigma - \epsilon)$ -relation, the **isophote twists** and the **minor axis rotation**.

Minor axis rotation can result from<sup>16</sup>:

- ▶ **projection effects** in triaxial systems or
- ▶ **misalignment** of the angular momentum and the shortest axis.

---

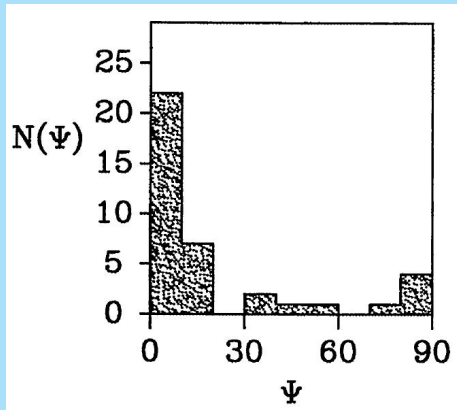
<sup>15</sup>J. Binney, Mon.Not.R.A.S. 183, 779 (1978)

<sup>16</sup>M. Franx, G. Illingworth & P.T. de Zeeuw, Ap.J. 383, 112 (1991)



We can *measure* the **apparent ellipticity**  $\epsilon$  and the **apparent misalignment**  $\psi$  (the ratio of maximum observed velocity on the apparent axes)

$$\tan \psi = \frac{v_{\min}}{v_{\max}}.$$



The distributions observed give the following rough indications:

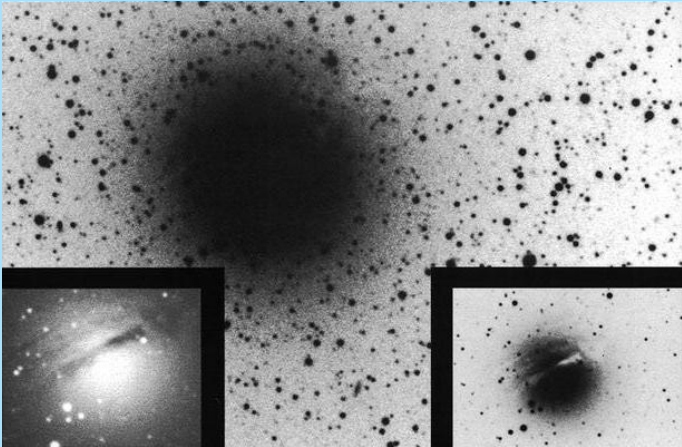
- ▶ Most (at least 50%) ellipticals have a small  $\psi_{\text{int}}$  ( $\lesssim 10^\circ$ ), but some ( $\approx 10\%$ ) rotate along their major axis.
- ▶  $\langle T \rangle \approx 0.3$  and  $T$  has a wide distribution with possibly as much as 40% of the galaxies prolate.
- ▶ The ratio  $c/a$  has a peak at about 0.6-0.7.

Dust lanes are often seen<sup>17</sup> and occur usually along the apparent minor axis, but also sometimes along the major axis.

---

<sup>17</sup>F. Bertola & G. Galletta, Ap.J. 226, L115 (1978)

Here is NGC 1947.



In triaxial potentials **stable orbits** are possible, but the detailed kinematics depends on the galaxy shape and body rotation.

In principle **dustlanes** can be used to determine the **intrinsic shape** of an individual galaxy <sup>18</sup>.

---

<sup>18</sup>R.L. Merritt & P.T. de Zeeuw, Ap.J. 267, L19 (1983); J. Kormendy & G. Djorkovski, Ann.Rev.A&A. 27, 235 (1989)

FIGURE ROTATION AXIS	TYPE OF ORBIT	DUST-LANE APPEARANCE	DUST-LANE KINEMATIC SIGNATURE
	Short	Equatorial	 Prograde
		Anomalous	 Perpendicular, then retrograde
	Long	Equatorial	 Retrograde
		Anomalous	 Perpendicular, then prograde

*Figure 1* Stable orbits of gas in a rotating triaxial galaxy (adapted from Merritt & de Zeeuw 1983). As illustrated, the figure tumbles in the direction of stellar rotation ( $\Omega_p > 0$ ); if  $\Omega_p < 0$ , the sense of gas rotation is reversed. Assume that the figure rotates about its shortest or longest axis (*left*). The second column gives the kind of orbit, and the third sketches resulting dust lanes seen edge-on. Anomalous orbits have different orientations at different radii (van Albada et al. 1982). They are the analogues of polar orbits in a stationary potential; at small radii, where  $\Omega_p$  is unimportant, they are polar. At large radii, the figure rotates several times during an orbit and so is effectively oblate-spheroidal; then the orbit is equatorial (Simonson 1982). In between, the orbits have skew orientations determined by the Coriolis force. The schematic illustrations of dust lanes show the directions of stellar and gas motion;  $\ominus$  indicates approach, and  $\oplus$  indicates recession. The right column states the kinematic signature, i.e. the sense of rotation of the dust lane with respect to the stars.

## Detailed kinematics

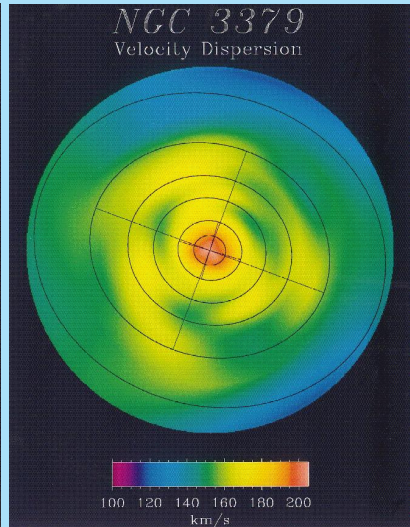
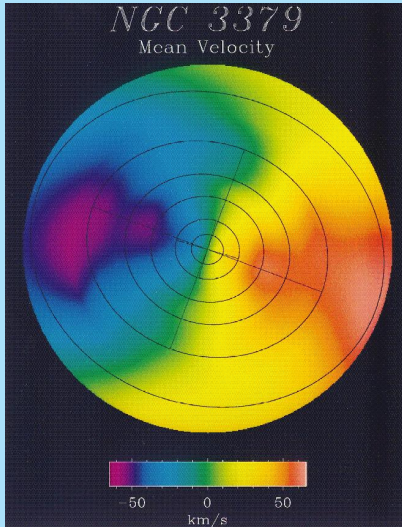
Detailed kinematics, including higher order moments, of the velocity distributions can now be observed.

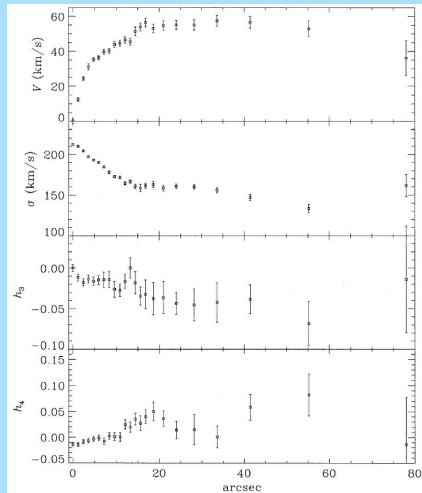
An example is a study of NGC3379<sup>19</sup>.

Dynamical modeling shows that NGC 3379 may be a flattened, weakly triaxial system seen in an orientation that makes it appear round.

---

<sup>19</sup>T.S. Statler & T. Smecker-Hane, A.J. 117, 839 (1999)

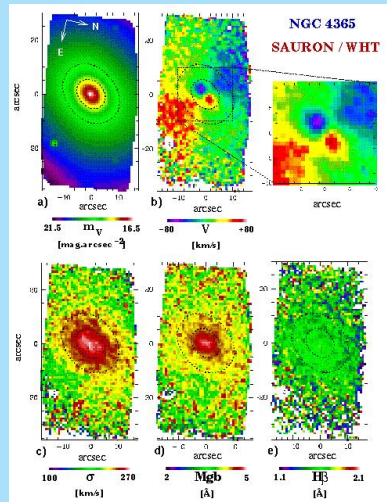




Recently the SAURON integral field spectrograph has been built and used to survey kinematics and structure of elliptical galaxies<sup>a</sup>.

---

<sup>a</sup>P.T. de Zeeuw et al.,  
Mon.Not.R.A.S. 329, 513 (2002)



## Central kinematics and black holes

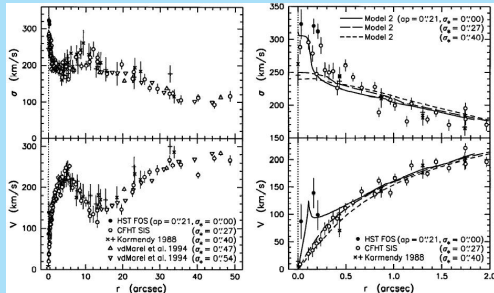
The central regions often show kinematics deviating from the outer parts.

These **distinct cores** may show:

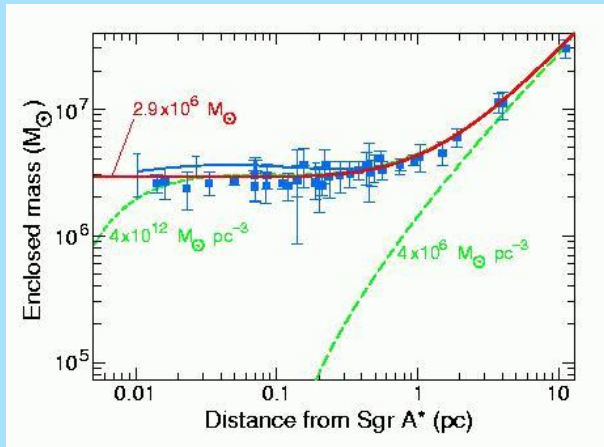
- ▶ **Rapid rotation in the core** but slow rotation in the main body
- ▶ **Opposite rotation in the core** relative to that in the main body
- ▶ **Core rotation along the minor axis.**

The **distinct cores** usually show small velocity dispersions, which suggest a **two-component galaxy** consisting of an elliptical with a small central **disk**.

Evidence for **black holes** comes from rapid rotation and high velocity dispersions in the inner regions, such as in **NGC 4594**<sup>20</sup> or **our own Galaxy**.



<sup>20</sup>J. Kormendy et al., Ap.J. 473, L91 (1996)

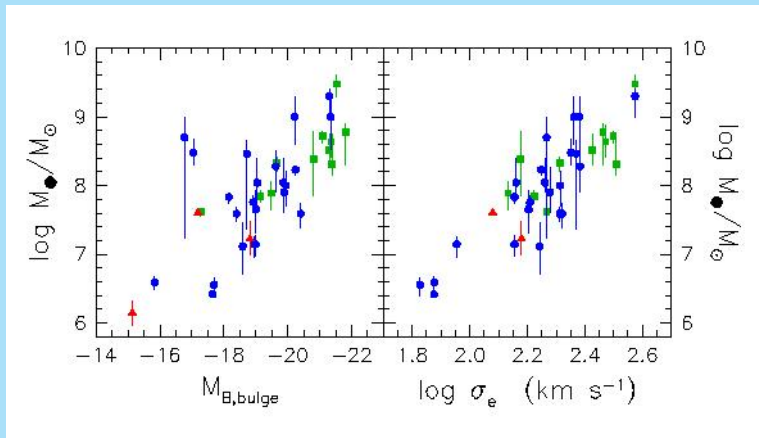


A compilation of all available data<sup>21</sup> shows a tight correlation between the **mass of the black hole** and the **luminosity** or **velocity dispersion** in the main body of the elliptical galaxy or bulge.

Probably this means no more than that larger galaxies have more material to feed into the center.

---

<sup>21</sup>S. Tremaine et al., Ap.J. 574, 740 (2002)



## Stäckel potentials

The most simple description is that of **King models**, which are isothermal spheres with tidal radii and truncations in the velocity distributions. For these we have can estimate the total mass from

$$\frac{M}{L} = \frac{9\sigma^2}{2\pi G I_0 r_c}.$$

However, we have seen that ellipticals have anisotropic velocity distributions and are in general triaxial.

A description then is with **Stäckel potentials**, which are potentials that are separable in **ellipsoidal coordinates**.

These are coordinates  $(\lambda, \mu, \nu)$  that are the three roots of  $\tau$  for

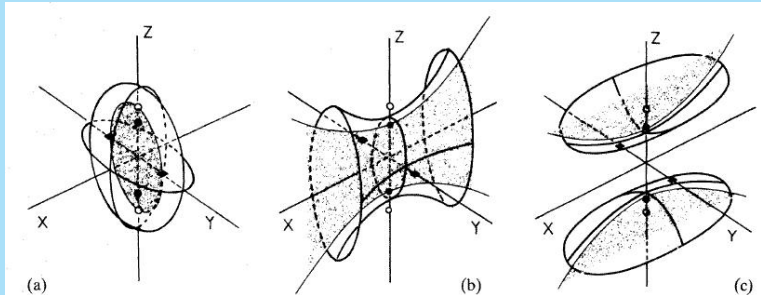
$$\frac{x^2}{\tau + \alpha} + \frac{y^2}{\tau + \beta} + \frac{z^2}{\tau + \gamma} = 1$$

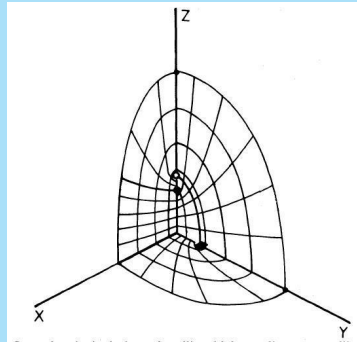
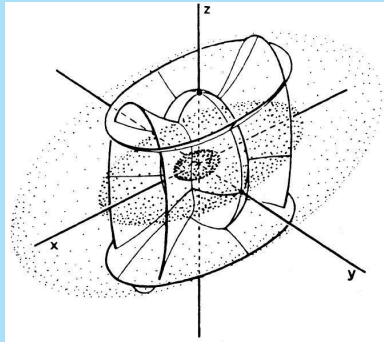
with  $\alpha < \beta < \gamma$  three constants.

In such coordinate systems surfaces of constant  $\lambda$  are **ellipsoids**, of constant  $\mu$  **hyperboloids of one sheet** and of constant  $\nu$  **hyperboloids of two sheets**.

These can be used to describe triaxial galaxies<sup>22</sup>.

<sup>22</sup>P.T. de Zeeuw, Mon.Not.R.A.S. 216, 273 (1985)





Stäckel potentials are of the form

$$\Phi(\lambda, \mu, \nu) = -\frac{F(\lambda)}{(\lambda - \mu)(\lambda - \nu)} - \frac{F(\mu)}{(\mu - \nu)(\mu - \lambda)} - \frac{F(\nu)}{(\nu - \lambda)(\nu - \mu)}$$

This can be used to describe triaxial galaxies<sup>23</sup>.

Many density distributions can be **locally approximated** with a Stäckel potential.

For example, it is possible to derive a **local approximation** to the the potential in a disk with a **flat rotation curve** by a Stäckel potential<sup>24</sup>.

<sup>23</sup>P.T. de Zeeuw & D. Lynden-Bell, Mon.Not.R.A.S. 215, 713 (1985); P.T. de Zeeuw, Mon.Not.R.A.S. 216, 273 (1985)

<sup>24</sup>T.S. Statler, Ap. J. 344, 217 (1989)

If the **density is specified on the z-axis** and if the potential is of the **Stäckel-form** in a specified **ellipsoidal coordinate system**, then the density at any point can be calculated with the so-called **generalized Kuzmin formula**<sup>25</sup>.

A set of models with **simple density profiles** has been calculated<sup>26</sup> to illustrate the usefulness.

A nice example is the **modified Hubble model**, which has

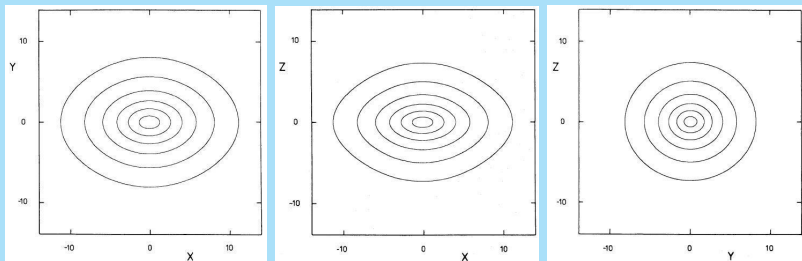
$$\rho(z) = \rho_0(1 + z^2)^{-3/2}$$

Then the coordinate system determines what the **axis ratio's** are in the density distributions and these change with radius.

<sup>25</sup>P.T. de Zeeuw, Mon.Not. R.A.S. 216, 599 (1985)

<sup>26</sup>P.T. de Zeeuw, R. Peletier & M. Franx, Mon.Not.R.A.S. 221, 1001 (1986)

Here are isodensity curves for a typical triaxial **modified Hubble model** (contour interval  $\log 3$ ).



So, this density distribution has smooth isodensity surfaces and has in a potential of **Stäckel form**!

## Dark matter

Solutions for **isotropic models** usually have gradients in  $M/L$ , while for **triaxial models** solutions with constant  $M/L$  are usually possible.

**X-ray halos** at large radii can also be used to measure masses of large ellipticals and clusters.

Measure the **emissivity** distribution  $\epsilon(r)$  from the distribution on the sky and the **temperature**  $T(r)$  from the energy distribution.

Infer from the distribution of  $\epsilon$  the **density** distribution of the gas  $\rho_{\text{gas}}(R)$ .

Then the hydrostatic equation gives for the **pressure**  $P$

$$\frac{dP}{dR} = -\frac{GM(< R)}{R^2} \rho_{\text{gas}}(R)$$

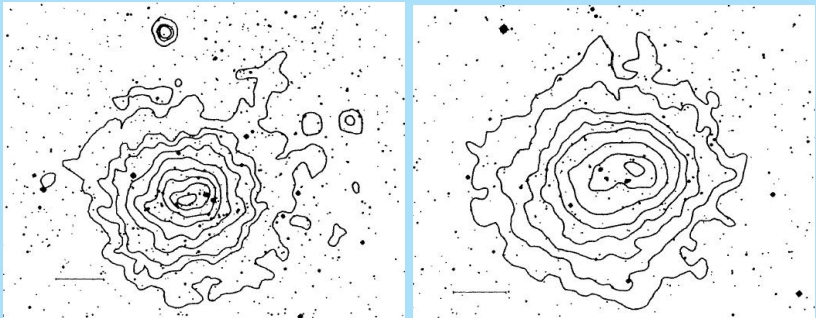
The ideal gas equation gives

$$P = \rho_{\text{gas}} \frac{kT}{\mu m_p}$$

Then

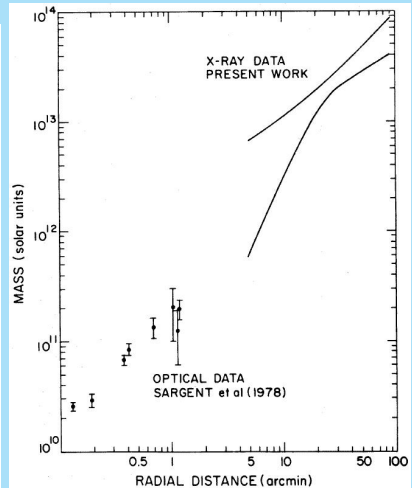
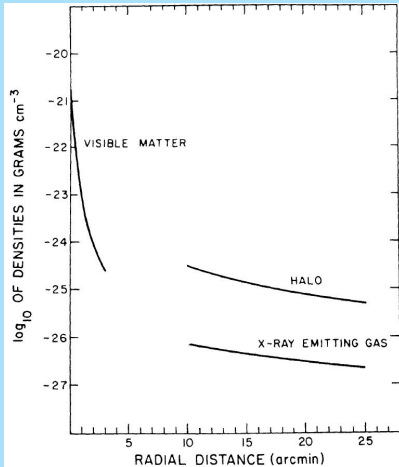
$$M(< R) = -\frac{kT(R)R}{G\mu m_p} \left[ \frac{d \log \rho_{\text{gas}}}{d \log R} + \frac{d \log T}{d \log R} \right].$$

Here are X-ray distributions in two clusters of galaxies.



The next two graphs show the analysis of the giant elliptical **M 87** in the center of the **Virgo cluster**<sup>27</sup>.

<sup>27</sup>Fabricant & Gorenstein, Ap.J. 267, 535 (1983)



**Shells** can also be used. Simulations show that their **spacing** depends on the mass profile.

Finally we can measure masses of whole **clusters** of galaxies.

The **Virial Theorem**  $2T + \Omega \sim 0$  for equilibrium for a uniform, spherical distribution gives

$$2T = \sum mV^2 \sim M\langle V^2 \rangle \sim -\Omega \sim \frac{3GM}{5R}$$

Thus

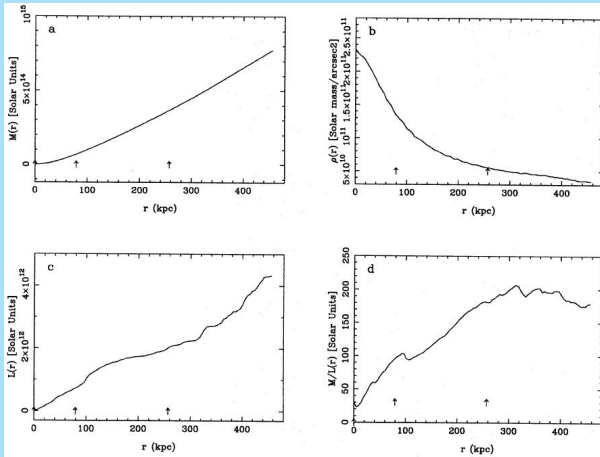
$$M \sim \frac{R\sigma_v^2}{G} \sim \left( \frac{R}{1 \text{ Mpc}} \right) \left( \frac{\sigma_v}{10^3 \text{ km s}^{-1}} \right)^2 10^{15} M_\odot$$

This indicates masses of up to  $10^{15} M_{\odot}$ .

Nowadays also gravitational arcs can be used<sup>28</sup>.



<sup>28</sup>e.g. in Abell 2218 by J.P. Kneib et al., A.&A. 303, 27 (1995)



# Formation

The oldest idea is that elliptical galaxies form through a **dissipative** process, where a relatively slowly contracting gas cloud forms stars and is slowly being enriched<sup>29</sup>.

This was thought to be the only way of getting color and metallicity gradients.

However, **color gradients should correlate with luminosity**, if the collapse is dissipative and this is not observed.

**Dissipational** collapse occurs when very early on a major fraction of the gas is turned into stars.

---

<sup>29</sup>R.B. Larson, Mon.Not.R.A.S. 166, 585 (1974) and 173, 671 (1975)

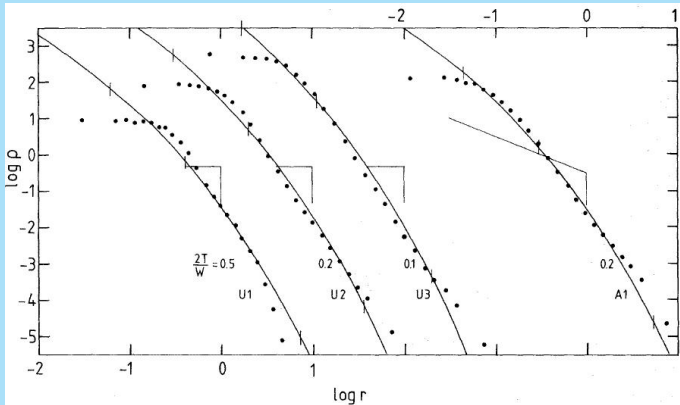
During the collapse **violent relaxation** takes place in the rapidly (relative to orbital periods) changing gravitational field.

**Van Albada**<sup>30</sup> was the first to simulate violent relaxation in numerical experiments.

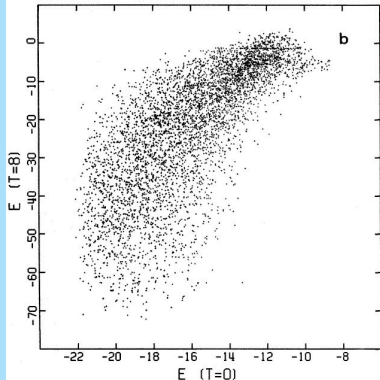
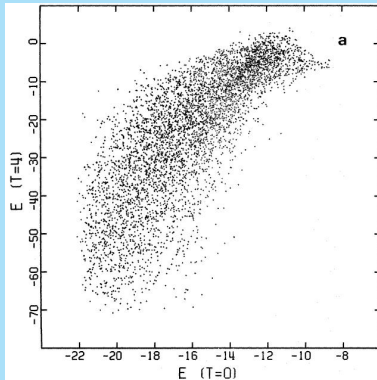
He found that for **irregular initial conditions** and **large collapse factors** an  **$R^{1/4}$ -law** results for the region containing between 10 and 99% of the mass.

---

<sup>30</sup>T.S. van Albada, Mon.Not.R.A.S. 210, 939 (1982)



He also found that the total energy of stars before and after collapse was correlated and therefore **color and abundance gradients can survive violent relaxation.**



In particular for giant ellipticals and cD's in clusters **merging** is likely to be important.

**The current observed rate of spiral mergers** (from interacting galaxies) **is high enough to produce the majority of ellipticals.**

**Merging** may be the cause of the following:

- ▶ The observed **low rotation in bright ellipticals.**
- ▶ The presence of **shells and ripples.**
- ▶ The occurrence of **kinematically distinct cores and multiple nuclei.**

Studies of clusters with central ellipticals with **multiple nuclei**<sup>31</sup> have been done, correcting the brightness distribution for the infalling galaxies.

This shows that a **merger rate** of up to **2 L\* per 5 × 10<sup>9</sup> years** is possible for the brightest cluster galaxies.

---

<sup>31</sup>e.g. T. Lauer, Ap.J. 325, 49 (1988)

